Journal of Neurotrauma
38:2999–3010 (November 1, 2021)
Mary Ann Liebert, Inc.
DOI: 10.1089/neu.2021.0151

Journal of Neurotrauma

In vivo Molecular Signatures of Cervical Spinal Cord Pathology in Degenerative Compression

Tomas Horak,[1–3] Magda Horakova,[1–3] Alena Svatkova,[4,5] Zdenek Kadanka Jr,[1,2] Petr Kudlicka,[1,3] Jan Valosek,[6,7] Tomas Rohan,[8] Milos Kerkovsky,[8] Eva Vlckova,[1–3] Zdenek Kadanka,[2] Dinesh K. Deelchand,[9] Pierre-Gilles Henry,[9] Josef Bednarik,[1–3] and Petr Bednarik[3,10,*]

Abstract

Degenerative cervical myelopathy (DCM) is a severe consequence of degenerative cervical spinal cord (CSC) compression. The non-myelopathic stage of compression (NMDC) is highly prevalent and often progresses to disabling DCM. This study aims to disclose markers of progressive neurochemical alterations in NMDC and DCM by utilizing an approach based on state-of-the-art proton magnetic resonance spectroscopy (^{1}H-MRS). Proton-MRS data were prospectively acquired from 73 participants with CSC compression and 47 healthy controls (HCs). The MRS voxel was centered at the C2 level. Compression-affected participants were clinically categorized as NMDC and DCM, radiologically as mild (MC) or severe (SC) compression. CSC volumes and neurochemical concentrations were compared between cohorts (HC vs. NMDC vs. DCM and HC vs. MC vs. SC) with general linear models adjusted for age and height ($p_{FWE} < 0.05$) and correlated to stenosis severity, electrophysiology, and myelopathy symptoms ($p < 0.05$). Whereas the ratio of total creatine (tCr) to total *N*-acetylaspartate (tNAA) increased in NMDC (+11%) and in DCM (+26%) and SC (+21%), myo-inositol/tNAA, glutamate + glutamine/tNAA, and volumes changed only in DCM (+20%, +73%, and −14%) and SC (+12%, +46%, and −8%, respectively) relative to HCs. Both tCr/tNAA and myo-inositol/tNAA correlated with compression severity and volume ($-0.376 < r < -0.259$). Myo-inositol/tNAA correlated with myelopathy symptoms ($r = -0.670$), whereas CSC volume did not. Short-echo ^{1}H-MRS provided neurochemical signatures of CSC impairment that reflected compression severity and clinical significance. Whereas volumetry only reflected clinically manifest myelopathy (DCM), MRS detected neurochemical changes already before the onset of myelopathy symptoms.

Keywords: cervical spinal cord, compression, degenerative; magnetic resonance; myelopathy; spectroscopy

Introduction

Degenerative changes in the spine develop with aging and frequently give rise to degenerative compression of the cervical spinal cord (CSC).[1] Magnetic resonance imaging (MRI) has revealed signs of CSC compression in 50% of randomly examined persons >60 years of age.[2] Prolonged compression often leads to clinically manifest degenerative cervical myelopathy (DCM).[3,4] However, in some patients, signs and symptoms of clinical myelopathy remain unexpressed, constituting a highly prevalent

[1]Faculty of Medicine, Masaryk University, Brno, Czechia.
[2]Department of Neurology, University Hospital Brno, Brno, Czechia.
[3]Multimodal and Functional Imaging Laboratory, Central European Institute of Technology, Brno, Czechia.
[4]Department of Medicine III, Clinical Division of Endocrinology and Metabolism, Medical University of Vienna, Vienna, Austria.
[5]Department of Imaging Methods, Faculty of Medicine, University of Ostrava, Czechia.
[6]Department of Neurology, Faculty of Medicine and Dentistry, Palacky University, Olomouc, Czechia.
[7]Department of Biomedical Engineering, University Hospital, Olomouc, Czechia.
[8]Department of Radiology, University Hospital Brno, Brno, Czechia.
[9]Department of Radiology, Center for Magnetic Resonance Research, University of Minnesota, Minneapolis, Minnesota, USA.
[10]Department of Biomedical Imaging and Image-guided Therapy, High Field MR Centre, Medical University of Vienna, Vienna, Austria.

*Address correspondence to: *Petr Bednarik MD, PhD, Department of Biomedical Imaging and Image-guided Therapy, High Field MR Centre, BT32, Medical University of Vienna, Lazarettgasse 14, 1090 Vienna, Austria E-mail:* petr.bednarik1@gmail.com

condition known as non-myelopathic degenerative compression (NMDC),[2] characterized by a variety of subclinical dysfunctional or microstructural impairments detectable by electrophysiological[5] or advanced MRI methods.[6,7] Unlike conventional MRI, proton magnetic resonance spectroscopy (^{1}H-MRS) quantifies neurometabolite levels and tracks changes in the cellular and biochemical composition of CSC tissue.[6–9] Thus, ^{1}H-MRS can provide markers specific to pathophysiological processes, such as gliosis, axonal/neuronal loss, and demyelination, resulting from mechanical compression.

Although only a few MRS studies have reported remote metabolic changes in the primary sensorimotor cortex arising out of CSC compression through Wallerian/Wallerian-like degeneration,[10,11] others have confirmed metabolic changes in the cranial CSC above the lesion level.[12–16] Increased levels of total creatine (tCr)/total N-acetylaspartate (tNAA)[11,12,15,17] and total choline (tCho)/tNAA[12,15,16] in DCM have also been reported. Higher spinal myo-inositol (myo-Ins)/tNAA and tCho/myo-Ins have been demonstrated in chronic CSC injury in diplegia and quadriplegia.[14] Studies to date have not included more than 35 participants[8,13,15] and often encountered technical challenges that compromised spectral quality. Metabolite changes have yet to be shown in the non-myelopathic stage.

We hypothesized that metabolite changes might be detected in NMDC by means of sensitive ^{1}H-MRS. More pronounced neurochemical impairment in DCM than in NMDC, and in severe compression (SC) than in mild compression (MC), could be anticipated. Given that SC is a condition with a greater risk that DCM will develop, the fact that MRS can distinguish between SC and MC becomes highly relevant to clinical practice.[18]

In view of this, MRS data were acquired from the cranial part of the CSC in the proximity of the stenosis in a large cohort (120 participants), using a fine-tuned 3 Tesla (T) MRS semi-LASER 3T sequence. The intention was to identify markers of CSC compression that might reflect progressive neurochemical deficits in groups defined by clinical (NMDC and DCM) or radiological (MC and SC) criteria when compared to healthy controls (HCs). The objective was to quantify the relationships between metabolite concentrations and CSC volume, and stenosis severity, together with electrophysiological and clinical outcomes.

Methods

Participant classification

Seventy-three participants with degenerative CSC compression and 47 HCs were enrolled between May 2018 and September 2019. All gave written informed consent. The local ethics committee approved the study (EKV-2017-055). Compression-affected participants were recruited by the University Hospital database. All participants underwent a clinical 1.5T MR scan (Philips-Achieva; Philips, Best, The Netherlands; Supplementary Materials S1.1.1) and the results were specialist screened for signs of CSC compression (Supplementary Materials S1.1.2)[2] and myelopathy.

Subjects without compression, cervical cord intensity changes on T_1- and T_2-weighted images, or any neurological symptoms or other illnesses were classified as HCs. Healthy persons were recruited to frequency match the age and sex of participants with compression. Expert neurological examination focused on clinical symptoms and signs of symptomatic myelopathy (Supplementary Materials S1.2). Participants with CSC compression were classified as non-myelopathic (NMDC) or exhibiting at least one clinical symptom and/or sign of myelopathy corresponding with a clinical diagnosis of DCM (Supplementary Table S1). Degree of disability and functional impairment was scored on the modified Japanese Orthopedic Association (mJOA) scale (3–18 points).[19]

Further, to detect functional abnormalities, electrophysiological measurements (Supplementary Materials S1.3) were taken of all participants with compression. Posterior columns or segmental lesions of the posterior horns were assessed with somatosensory-evoked potentials (SEP), dysfunction of the corticospinal tracts with motor-evoked potentials (MEP), and segmental lesions of the anterior horns with electromyography (EMG).[20,21]

Maximum compression level (MCL) was consensually determined by two specialists (T.R., M.H.); compression was quantified at MCL as both cross-sectional CSC area (CSA) and compression ratio (CR). The C4/5 level was used as a reference in HCs. Groups were established on the basis of the radiological severity of CSC compression at MCL: MC (CR $\geq$0.4 or CSA $\geq$70.1 mm^2) and SC (CR $<$0.4 and CSA $<$70.1 mm^2).[22]

Magnetic resonance data acquisition at 3 Tesla

MRS data were acquired on a 3T scanner (Siemens-Prisma; Siemens Healthcare, Erlangen, Germany) with a standard 64-channel head-neck coil, in separate sessions. The subject's neck was fixed with a memory foam collar.[23] High-resolution ($0.6\times0.6\times3$ mm, repetition time [TR] = 3500 ms, and echo time [TE] = 106 ms) T_2 turbo spin echo (TSE) images were obtained to center the 3.2-mL ($8\times9\times45$ mm) MRS voxel posterior to vertebra C2 (Fig. 1), that is, above the compression level in subjects with CSC compression. Magnetic field inhomogeneities were minimized by means of fast, automatic shimming technique by mapping along projections.[24] MRS data were acquired with a cardiac-triggered sLASER (256 single shots; TR = 5 sec, TE = 28 ms, acquisition time $\sim$21 min, scanner sofware version: syngo VE 11C, number of complex points: 2048, frequency offset of MRS acquisition: - 2 ppm, sweep width: 6000 Hz, location of outer volume suppression [OVS] bands: X, Y, Z, the width of OVS slabs 120 mm); water was suppressed with frequency-selective variable pulse power and

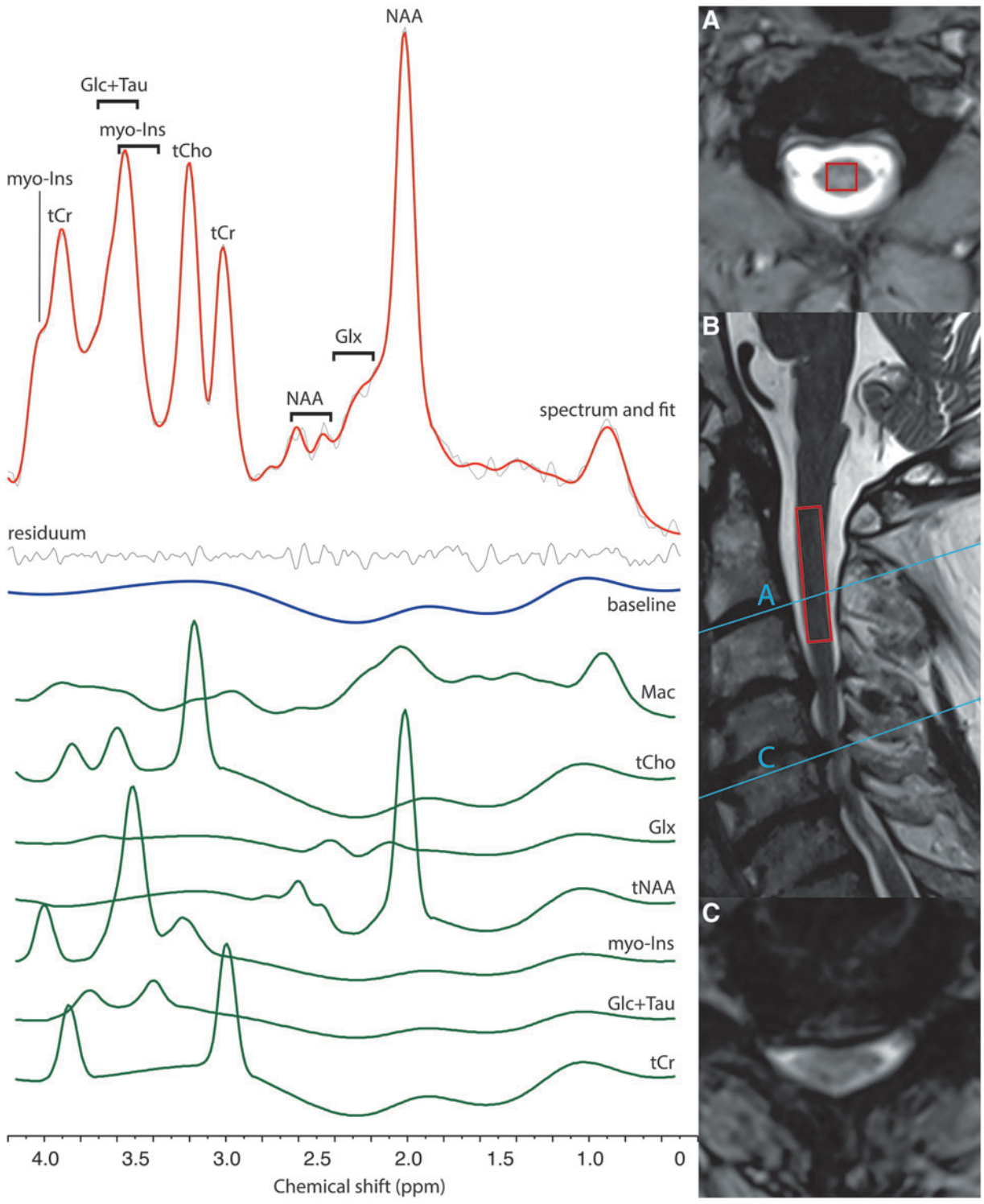

FIG. 1. Example of an MR spectrum and its quantification in LCmodel. Data were obtained from the cervical spinal cord of 1 healthy volunteer. Voxel position is shown on a sagittal T_2-weighted MR image (inset). Blue A and C letters on (**B**) represent the positions of axial/transverse slices of (**A**) and (**C**). MR, magnetic resonance; Mac, macromolecules; Cr, creatine; Glc, glucose; Glx, glutamate + glutamine; myo-Ins, myo-inositol; Lac, lactate; NAA, N-acetylaspartate; Tau, taurine; tCho, total choline; tCr, total creatine; tNAA, total N-acetylaspartate. Color image is available online.

optimized relaxation delays water suppression,[25] and fat and water signals originating outside the MRS voxels were suppressed by the OVS.[23]

Hyperbolic secant adiabatic pulses[26] were replaced by frequency-offset corrected inversion (bandwidth 50 kHz) refocusing pulses for improved semi-LASER localization performance.[27]

Magnetic resonance imaging/magnetic resonance spectroscopy data processing

T_2-TSE images were segmented automatically using Spinal Cord Toolbox v3.2.3[28] to create CSC masks for volumetry and cerebrospinal fluid (CSF) fraction calculations, both measured in the segment covered by the MRS voxel.

MR spectra were saved as single shots and processed in MRspa (Magnetic Resonance signal processing and analysis, Center for Magnetic Resonance Research, University Of Minnesota, USA). Metabolite spectra were summed in blocks of 8 (32×8 per subject), corrected for frequency and phase drifts and the residual effects of eddy currents, and summed to obtain spectrum for single-subject analysis. MR spectra from each subject were pooled and summed to obtain one group-averaged spectrum with high signal-to-noise ratio (SNR) for each of the cohorts. Spectral SNR and linewidths were provided by LCmodel based on metabolite spectra analysis.

Single-subject and group-averaged spectra were analyzed in LCmodel v6.3-0G[29] utilizing a basis set, which included a measured spectrum of macromolecules (Mac)[30] and simulated spectra of 18 metabolites.[31] Metabolites were quantified as ratios to tNAA. Although the pulsatile flow of the CSF can be partially compensated by ECG trigger,[32–34] absolute quantification through internal water referencing is rendered unreliable by biased quantification of the water spectrum in CSC.[14] Quality-control criteria based on Cramér-Rao lower bounds (CRLB) and correlation coefficients provided by LCmodel (R_L) served to select reliably-quantifiable metabolites (Supplementary Materials S1.4).[23]

Statistical analysis

Data were analyzed in SPSS software (v25; IBM Corp., Armonk, NY). Based on the Kolmogorov-Smirnov test, continuous variables with normal and non-Gaussian distribution are presented as means ± standard deviation (SD) and medians (5th–95th percentile), respectively. Demographic and physical parameters were compared between groups by means of the parametric *t*-test/analysis of variance (ANOVA) or the non-parametric Mann-Whitney/Kruskal-Wallis for continuous variables, with chi-square tests for categorical variables. Spearman's correlations assessed relationships between selected continuous variables.

General linear models corrected for the effects of age and height, with *post hoc* tests, were used for between-group comparison of single-subject metabolite ratios and CSC volumes. The Bonferroni correction was applied to correct type 1 errors in *post hoc* group comparisons. Uncertainty intervals of metabolite ratios obtained from the quantification of group-averaged MR spectra were propagated from the CRLB of each metabolite as fractional uncertainties. Thus, between-group differences were considered significant when intervals given by propagated errors did not overlap.

Partial correlations, controlled for age and height, were performed separately for HCs and subjects with compression to assess the relationship between metabolite ratios, CSC volumes, CSA, and CR.

Results

Demographics, physical characteristics, confounding variables

Age, sex, height, weight, and body mass index did not differ significantly within HC, NMDC, and DCM, nor between HC, MC, and SC. However, patients with DCM were, on average, 4 years older than those with HC (Table 1). Analysis revealed that height was a factor that influenced MRS and volumetry outcomes (Supplementary Materials S2.1). Different spinal segments were involved, to a variable extent, in MRS and volumetry assessment, a trend arising out of variable subject height

Table 1. Basic Characteristics of Study Cohort

Group	N	*Sex*	*Age: women (years)*	*Age: men (years)*	*Height (cm)*	*Weight (kg)*	*Body mass index (kg/m²)*	*Linewidth (Hz)*	*Signal-to-noise ratio*
HC	47	F 57.4%	53.6 ± 10.5	53.1 ± 7.8	173.3 ± 10.4	80.1 ± 15.7	26.6 ± 4.3	12.1 (8.5, 18.7)	13.0 (9.4, 16.6)
NMDC	60	F 51.7%	54.9 ± 10.8	55.2 ± 9.7	171.5 ± 9.0	81.4 ± 16.3	27.5 ± 3.9	12.6 (6.6, 17.1)	13.0 (9.0, 19.0)
DCM	13	F 46.2%	57.4 ± 7.5	57.9 ± 16.2	169.8 ± 7.0	82.1 ± 15.7	28.4 ± 4.9	11.9 (9.6, 17.6)	14.0 (10.0, 17.6)
Sig.		$p = 0.720$	$p = 0.696$	$p = 0.516$	$p = 0.405$	$p = 0.887$	$p = 0.302$	$p = 0.812$	$p = 0.570$
MC	41	F 41.5%	55.9 ± 9.9	56.6 ± 8.9	172.4 ± 8.2	82.9 ± 15.3	27.7 ± 3.8	12.7 (6.6, 17.8)	13.0 (8.1, 18.0)
SC	32	F 62.5 %	54.8 ± 10.9	54.0 ± 14.7	169.6 ± 9.2	79.8 ± 17.1	27.5 ± 4.5	11.6 (8.5, 19.0)	14.0 (9.7, 19.7)
Sig.		$p = 0.160$	$p = 0.761$	$p = 0.485$	$p = 0.213$	$p = 0.635$	$p = 0.384$	$p = 0.394$	$p = 0.731$

Values are presented as mean ± SD or median (5th, 95th percentile interval), except where indicated as percentage (%). The *p* values are derived from the chi-square test for sex and ANOVA/Kruskal-Wallis tests for continuous variables.

HC, healthy controls; NMDC, non-myelopathic degenerative compression; DCM, degenerative cervical myelopathy; Sig, significance; MC, mild compression; SC, severe compression; F, female; SD, standard deviation; ANOVA, analysis of variance.

and the constant length of the MRS voxel.[35] Because it was considered impossible to rule out the effects of bias intrinsic to age and height in the between-group differences in metabolite levels and volumes, age and height were introduced as covariates. Because there was no between-subject difference ($p > 0.15$) in metabolite ratios with MCL at C3/4 ($N = 5$), C4/5 ($N = 20$), C5/6 ($N = 35$), and C6/7 ($N = 13$; Table 2), MCL was not considered a confounding factor.

Magnetic resonance spectroscopy data quality

Linewidth of unsuppressed water spectra measured in MRSpa software was 12.4 (8.2, 17.8) Hz. The LCmodel provided linewidth and SNR of 13.7 (9.7, 19.6) and 13.0 Hz (9.1, 18.0), respectively, as measured on metabolite spectrum. These parameters did not differ between groups (Table 1). The LCmodel quantified metabolites with CRLB medians below 10% for Mac, myo-Ins, tCho, tCr, and tNAA, and below 30% for glucose (Glc) + Tau and combined glutamate/glutamine (Glx) in single-subject spectra analysis, whereas the CRLB of group spectra were 5% for Mac, 3–4% for tCr, 11–15% for Glc + Tau, 10–13% for Glx, 2% for myo-Ins, 4–5% for tCho, and 2–3% for tNAA.

Single-subject magnetic resonance spectra quantification

Between-group differences and their significance appear in Figure 2A (groups based on clinical terminology) and in Figure 2B (groups based on radiological terminology), whereas their averages appear in Table 3. NMDC patients showed altered myo-Ins/tNAA compared to DCM ($p = 0.009$) and tCr/tNAA compared to HCs ($p = 0.003$). Further, tCr/tNAA ($p < 0.001$), Glx/tNAA ($p = 0.010$), and myo-Ins/tNAA ($p = 0.001$) were higher in DCM than in HCs. Differences in tCr/tNAA between the two patient groups (NMDC vs. DCM) and any tCho/tNAA deficits that appeared between patients and HCs did not pass Bonferroni's correction.

Single-subject spectra analyses also revealed differences in tCr/tNAA ($p < 0.001$), Glx/tNAA ($p = 0.001$), and myo-Ins/tNAA ($p = 0.001$) between HC and SC as well as between MC and SC in tCr/tNAA ($p < 0.001$), Glx/tNAA ($p = 0.004$), and myo-Ins/tNAA ($p = 0.006$). Distinctly different tCho/tNAA ($p = 0.011$) levels were found between HC and SC. Alterations in Mac/tNAA and Glc + Tau/tNAA between groups based on compression severity did not pass correction for type 1 error (Supplementary Table S2).

Group-averaged magnetic resonance spectra

High-SNR group averages of MR spectra served for visual comparison of the distinctive spectral patterns that appear in Figure 3, whereas their quantification yielded concentrations with higher accuracy than that of lower-SNR single-subject spectra (Fig. 2). Comparison with HC revealed significantly higher tCr/tNAA and myo-Ins/tNAA in both NMDC and DCM, whereas Glx/tNAA and Glc + Tau/tNAA were only elevated in DCM, as was tCho/tNAA in NDCM. Significant differences in tCr/tNAA, Glx/tNAA, myo-Ins/tNAA, and tCho/tNAA were detected in both groups defined by compression severity, with more profound deficits in SC compared to MC, whereas differences between MC and SC patients emerged in Mac/tNAA (Table 3).

Segmentation outcomes

Significant reductions in CSC volume in DCM compared to HC ($-412\,mm^3$; -14%) and compared to NMDC ($-363\,mm^3$; -12%) were observed (Fig. 4). In contrast to metabolite ratios, differences in volumes between HC and NMDC were not significant. CSC volumes were also significantly lower in SC than in HC ($-250\,mm^3$; -8%) and in SC than in MC ($-213\,mm^3$; -7%), whereas differences between MC and HC were non-significant (Table 2). The within-voxel CSF fraction was significantly higher in DCM (38.5% [27.4, 57.7]) compared to HC (27.3% [14.5, 33.5]; $p < 0.0001$) and NMDC (27.3% [16.0, 39.2]; $p < 0.0001$) and in SC (31.5% [19.0, 54.3]) compared to HC ($p < 0.0001$) and MC (25.2% [16.2, 43.8]; $p < 0.0001$).

Table 2. Radiological Characteristics of the Study Cohort

Group	*CR*	*CSA (mm^2)*	*Volume (mm^3)*	*MCL at C3/4*	*MCL at C4/5*	*MCL at C5/6*	*MCL at C6/7*
HC	0.52 (0.41, 0.64)	72 (61, 85)	3024 (2501, 3693)	n.a.	n.a.	n.a.	n.a.
NMDC	0.41 (0.28, 0.54)	62 (43, 88)	2975 (2448, 3480)	4 (7%)	17 (28%)	26 (43%)	13 (22%)
DCM	0.36 (0.24, 0.48)	53 (26, 74)	2612 (1096, 2953)	1 (8%)	3 (23%)	9 (69%)	0 (0%)
Sig.	$p = 0.009$*	$p = 0.013$*	$p < 0.001$*		—		
MC	0.45 (0.38, 0.59)	68 (43, 88)	2987 (2524, 3636)	3 (7%)	10 (24%)	21 (51%)	7 (17%)
SC	0.35 (0.24, 0.39)	54 (28, 67)	2774 (1777, 3367)	2 (6%)	10 (31%)	14 (44%)	6 (19%)
Sig.	$p < 0.001$*	$p < 0.001$*	$p < 0.001$*		—		

Compression ratio (CR) and cross-sectional areas (CSA) measured at maximum compression level (MCL), as well as spinal cord volumes measured above the compression level, are presented as medians (5th, 95th percentile intervals). The p values are derived from Kruskal-Wallis tests for continuous variables and chi-square tests for MCL. An asterisk (*) indicates $p < 0.05$. The number of participants with different MCLs and their proportional representation within the groups compared are summarized in the left part of the table.

HC, healthy controls; NMDC, non-myelopathic degenerative compression; DCM, degenerative cervical myelopathy; Sig, significance; MC, mild compression; SC, severe compression; n.a., not applicable.

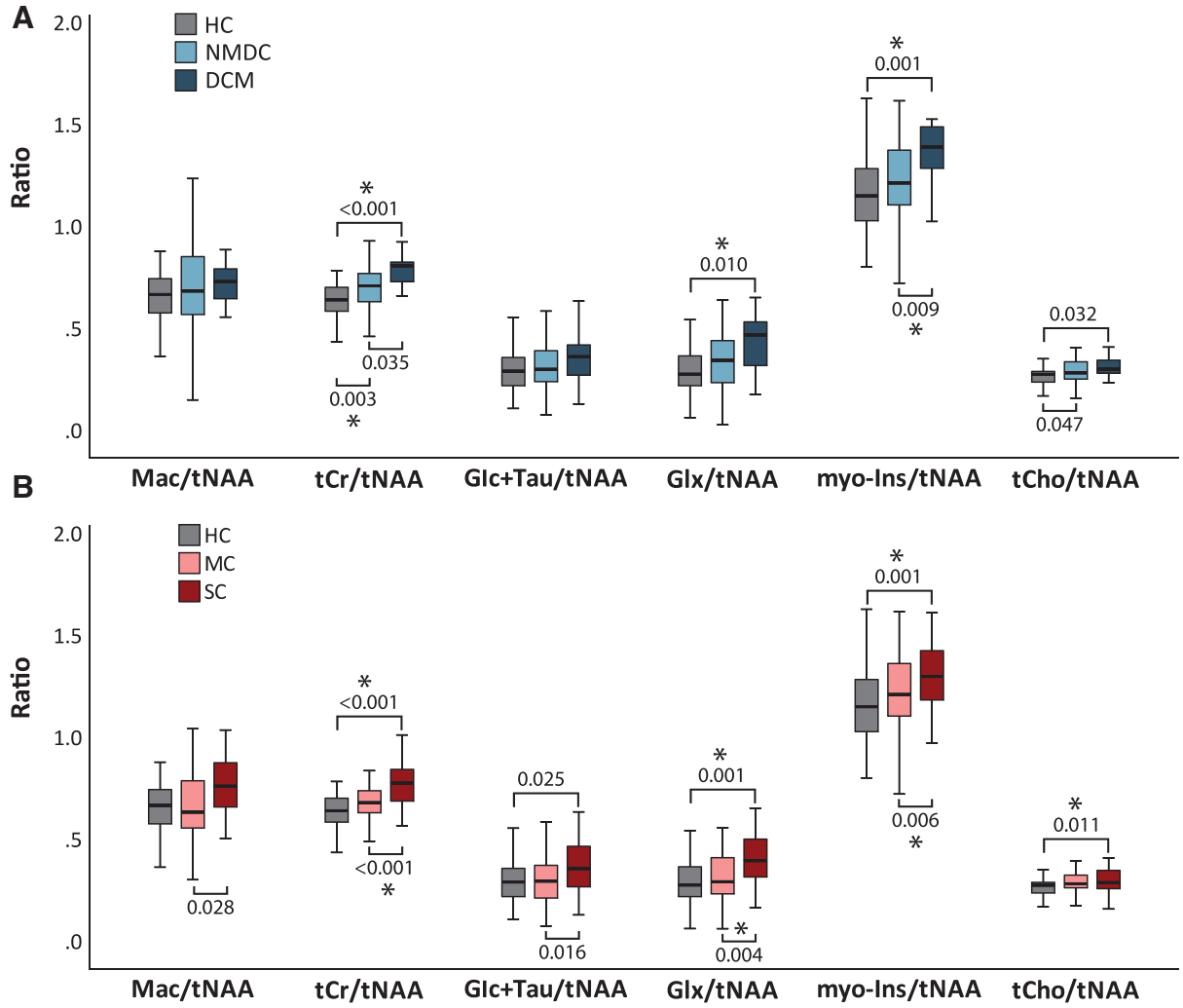

FIG. 2. Single-subject MR spectra quantification. Between-group comparison (general linear model corrected for age and height) of metabolite ratios in healthy controls (HC; $N=47$) and subjects with non-myelopathic degenerative compression (NMDC; $N=60$) and degenerative cervical myelopathy (DCM; $N=13$; **A**) and HC and subjects with mild compression (MC, $N=41$) and severe compression (SC; $N=32$) (**B**). Numbers represent p values uncorrected for multiple comparisons. Asterisks indicate significant differences that passed Bonferroni's correction. Bars represent 25th–75th percentiles; whiskers denote the lowest and highest values, excluding outliers (values >1.5 times the interquartile range). Medians appear as horizontal lines within the bars. MR, magnetic resonance. Color image is available online.

Relationship between neurochemistry, compression severity, cervical spinal cord volumes, and electrophysiology

The relationships between CR and CSA (at MCL), volume, and selected neurochemical levels appear in Table 4 and Supplementary Figure S2. Physiological correlations in HCs are shown together with correlations in compression-affected subjects. Whereas correlations of tCr/tNAA, Glx/tNAA, and myo-Ins/tNAA with volume, CSA, and CR were consistently negative in compression, opposite, positive, relationships between tCr/tNAA, myo-Ins/tNAA, and radiological measures were observed in HCs.

Although significant correlations ($p<0.0001$) between CSC volume and CSA were found in both HCs ($r=0.643$) and compression-affected subjects ($r=0.681$), the correlation between CSC volume and CR significance was confined to subjects with compression ($r=0.363$, $p=0.002$), but was not attained in HCs ($r=-0.156$, $p=0.306$). The relationship between neurochemistry and

Table 3. Between-Group Differences from LCmodel Analysis of Single-Subject (Single-SUBJ) and Group-Averaged (Group-AVG) Spectra

Metabolite	*Mac/tNAA (%)*		*tCr/tNAA (%)*		*Glc + Tau/tNAA (%)*		*Glx/tNAA (%)*		*myo-Ins/tNAA (%)*		*tCho/tNAA (%)*	
Difference	*Single-subject*	*Group-avg.*	*Single-subject*	*Group-avg.*	*Single-subject*	*Group-avg.*	*Single-subject*	*Group-avg.*	*Single-subject*	*Group-avg.*	*Single-subject*	*Group-avg.*
NMDC - HC	3.2	1.2	11.0	12.6	3.1	12.5	31.6	13.8	5.6	6.9	3.7	13.1
DCM - HC	10.9	8.0	25.6	14.4	24.0	33.9	72.9	32.9	19.9	11.3	10.0	6.4
DCM - NMDC	7.5	6.8	13.2	1.6	20.2	19.0	31.4	16.8	13.5	4.1	6.1	–5.9
MC - HC	–5.3	–3.3	8.0	11.0	1.4	6.6	11.2	4.3	5.7	6.7	4.1	11.2
SC - HC	15.5	9.6	21.0	9.6	22.2	29.8	45.7	39.6	12.4	8.0	4.8	9.1
SC - MC	22.0	13.0	12.1	–1.2	20.5	21.8	31.1	33.8	6.3	1.2	0.7	–1.9

Average differences from single-SUBJ data analysis are compared with differences resulting from the analysis of group-AVG spectra. Whereas light red indicates that significance that did not pass correction for multiple comparison, dark red highlights differences significant after multiple comparison correction. Statistical comparison was performed with a general linear model corrected for age and height effects and *post hoc* tests. In group-averaged MR spectra, the significance of the differences was assessed by means of the intervals given by estimated quantification errors (Cramer-Rao lower bounds). Gray cells mark differences lying where error intervals did not overlap. Color table is available online.

HC, healthy controls; NMDC, non-myelopathic degenerative compression; DCM, degenerative cervical myelopathy; MC, mild compression; SC, severe compression; Mac, macromolecules; tNAA, total *N*-acetylaspartate; tCR, total creatine; Glc, glucose; Glx, combined glutamate/glutamine; myo-Ins, myo-inositol; tCho, total choline; MR, magnetic resonance.

electrophysiology can be found in the Supplementary Materials (Supplementary Materials section S2.3 and Supplementary Fig. S1), together with electrophysiological characteristics of the study cohorts (Supplementary Table S3). For relationship between radiological characteristics and neurometabolites, see Supplementary Figure S2.

Relationship between neurochemistry, volumetry, and myelopathy symptoms

According to the mJOA[19] score, with a median of 16 (9, 17), most of the DCM patients (8 of 13) were classified within mild myelopathy. A significant correlation between mJOA and myo-Ins/tNAA ($r=-0.665$, $p=0.013$) appeared (Fig. 5). Because of the relatively low number of DCM patients ($N=13$), the correlation between mJOA and neurochemicals was not corrected for height. The observed significant correlations between mJOA and Mac/tNAA ($r=-0.623$, $p=0.023$) might therefore be a consequence of the height effect on Mac/tNAA levels (Supplementary Materials S2.1). Correlation between volumes and mJOA was not significant ($r=0.192$, $p=0.531$).

Discussion

Our study identified metabolic alterations in spinal neurochemical profiles of distinct compression phenotypes. Revealed distinctions in metabolite fingerprints between subclinical degenerative compression and HCs imply high sensitivity of the methodology. Sensitive metabolic markers are required for longitudinal studies to estimate risk of the development of myelopathy and reveal potential candidates for preventive decompressive surgery among patients without myelopathy symptoms. Such predictors may well revolutionize clinical practice in terms of anticipative protocols; however, longitudinal studies are needed to verify the assumption. This MRS study benefited from the full-signal-intensity semi-LASER pulse sequence, fine-tuned by implementing broadband frequency-offset corrected inversion pulses, leading to a reduction in undesired lipid signals from vertebrae. Further, this approach minimized chemical shift displacement error and attenuated J-evolution/T_2-relaxation relative to point-resolved spectroscopy (PRESS).[27] Spectral quality consistent across the study facilitated the reliable quantification of 10 metabolites, in similar fashion to recent outcomes with metabolite-cycled PRESS.[14]

High spectral quality facilitated the capture of early alterations in tCho/tNAA and tCr/tNAA in NMDC, and more profound differences in tCr/tNAA, myo-Ins/tNAA, Glx/tNAA, and tCho/tNAA in DCM, when compared to HCs. These outcomes prevail over clinical MRI findings, which are unable to distinguish between NMDC and DCM and adequately to reflect clinical status in CSC compression.[36] Total Cr/tNAA, myo-Ins/tNAA, Glx/tNAA, and Glc + Tau/tNAA ratios differed significantly between subjects with MC and SC, likely because NMDC subjects with SC are at higher risk of DCM development.[2] Thus, the distinctions in tCr/tNAA and tCho/tNAA found between NMDC and HC arose out of more-severe compressions in certain subjects.

LCmodel analysis of single-subject spectra was corroborated by the quantification of spectral sums by group. The resulting values were compared while accounting for quantification errors, that is, LCmodel-provided CRLBs of individual metabolites propagated to the ratios. Despite the intrinsic statistical distinctions between the two comparison approaches, the higher SNR of group averages improved quantification accuracy for the metabolites and confirmed the key findings of single-subject spectra analyses. Both comparisons clearly show the dependence of tCr/tNAA, myo-Ins/tNAA, and tCho/

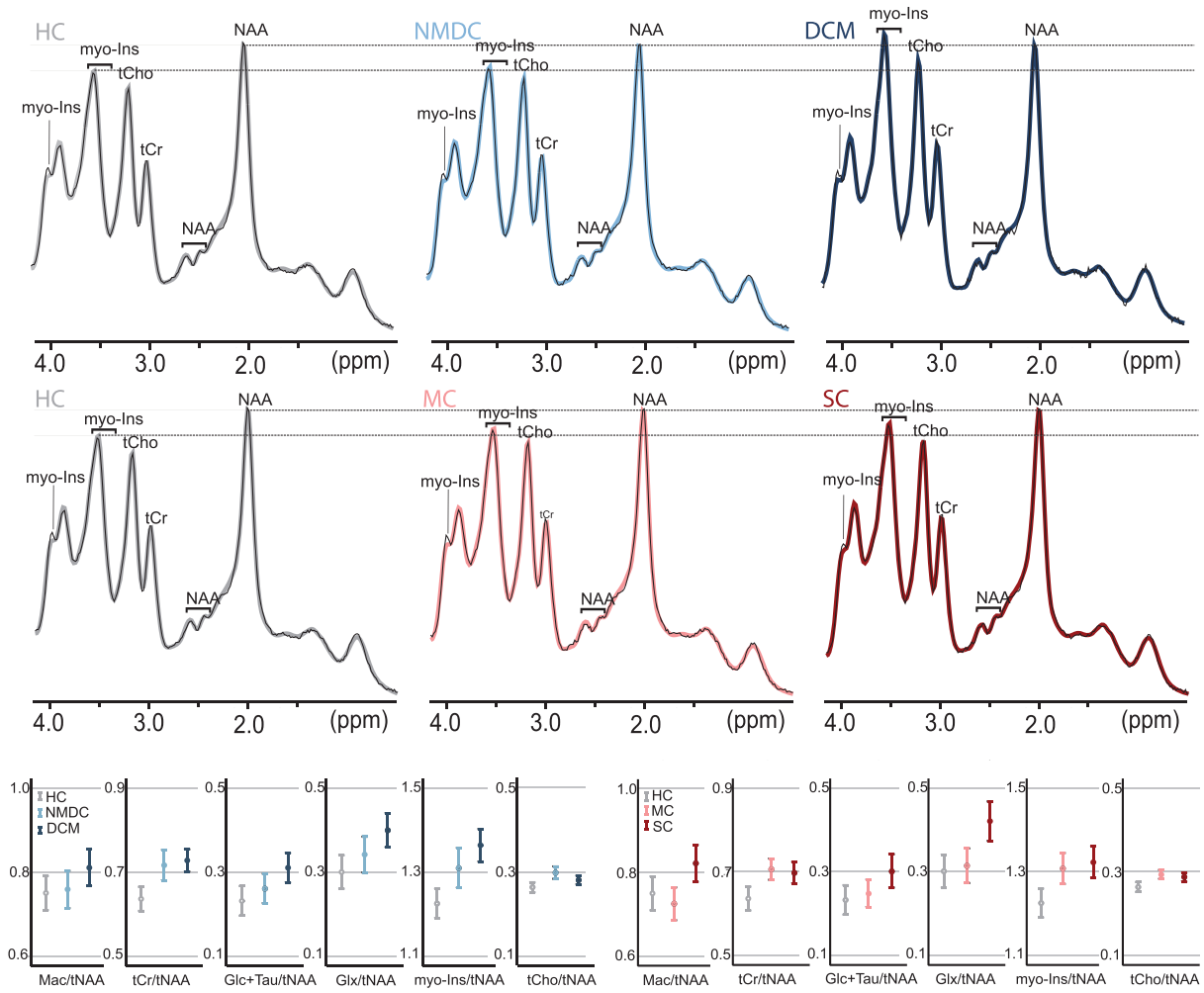

FIG. 3. Group-averaged MR spectra and their quantification in LCmodel. Spectra of individual subjects were pooled and summed, whereas group averages for healthy controls (HC; $N=47$) were compared to spectra representing non-myelopathic degenerative compression (NMDC; $N=60$) and degenerative cervical myelopathy (DCM; $N=13$; **A**) and to spectra representing mild compression (MC; $N=41$) and severe compression (SC; $N=32$; **B**). The spectra (black line) and their LCmodel fits (in color) are scaled using NAA-methyl resonance at 2 ppm. Horizontal lines indicate height of 2 ppm NAA-methyl peak (upper), 3.56 ppm myo-Ins peak, and 3 ppm Cr-peak in HC to facilitate visual comparison. Outcomes of quantification in LCmodel are shown in plots (**C**), where error bars represent Cramer-Rao lower bounds propagated to the ratio of metabolites. MR, magnetic resonance; myo-Ins, myo-inositol; NAA, *N*-acetylaspartate. Color image is available online.

tNAA on the radiological severity of compression and clinical impairment. Both methods disclosed differences in tCr/tNAA and tCho/tNAA between HC and NMDC, largely driven by SC subjects. Therefore, early signatures of spinal neurochemical impairment merit future longitudinal studies to improve the stratification of patients with cervical compression and their subsequent management.

Although degenerative stenosis precluded consistent voxel placement at the compression level, metabolite changes propagate rostrally from the CSC lesion up to the brain through Wallerian/Wallerian-like neurodegeneration.[11,17,37] Myo-Ins/tNAA elevation, which reflects neuronal/axonal loss or demyelination (tNAA)[38] and gliosis or inflammation (myo-Ins), accords with recent MRS work on chronic spinal cord injury[14] and other studies of neurodegeneration.[39–41] Elevated tCho and tCho/tNAA have indicated increased membrane turnover arising out of ongoing neurodegeneration/demyelination[39] and have been associated with the duration of spinal cord injury.[14] Increased tCr/tNAA and Glx/tNAA ratios attributable to compression might relate to various pathophysiological processes.

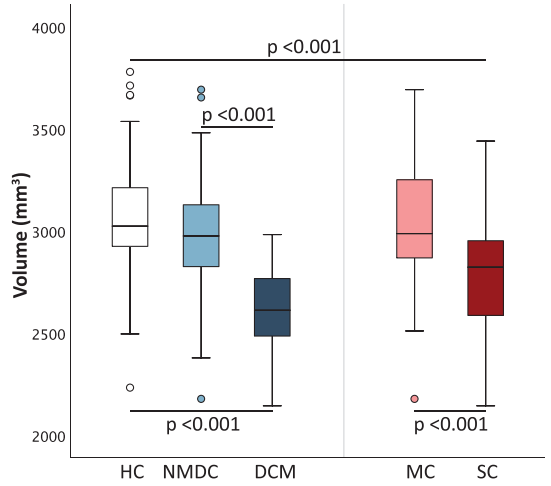

FIG. 4. Volumes of cropped individual spinal cord masks calculated above the level of stenosis, beginning with the slice corresponding to the bottom edge of vertebra C3, taking 90 cranial slices into account. The *p* values are derived from general linear models corrected for age and height. The bars represent the 25th–75th percentiles; whiskers denote the lowest and highest values, with the exception of outliers (values >1.5 times the interquartile range), which are marked as circles. Medians appear as horizontal lines within the bars. NAA, *N*-acetylaspartate. Color image is available online.

Although exact interpretation is challenging, particularly because individual metabolites (e.g., creatine and phosphocreatine) cannot be reliably separated, the changes might be driven by decreased tNAA and related to neurodegeneration/demyelination. Both tCr and tCho were quantified with relatively high accuracy, leading to low SDs in tCr/tNAA and tCho/tNAA, reflecting early reduction in tNAA. In contrast, tCho/myo-Ins was not significantly altered in patients with chronic CSC injury,[14] probably attributable to limited, not fully developed neurochemical changes in substantially milder CSC impairment. The contrasting relationship between neurochemicals and volume in HCs and subjects with compression implies that neurochemical levels reflect altered CSC composition rather than atrophy. The CSF fraction did not bias metabolite ratios within the MRS voxel; the relevant metabolites (except for Glc) are not measurable in CSF. In accord with earlier publications,[7,42] the degree of rostral CSC atrophy correlated with the degree of compression.[11] In contrast to the situation with neurochemicals, CSC volume was not significantly different between HC and NMDC. This suggests that volumetry reflects more-severe CSC impairment and is less sensitive than MRS to early changes.

The significant correlation between mJOA and myo-Ins/tNAA highlights the capacity of MRS to reflect the degree of clinical severity and serve as a potential predictor of DCM development.[17,36]

The current work was limited by the relatively low number of participants in the DCM group; this condition is relatively rare compared with NMDC,[2] and DCM patients are difficult to recruit because urgent surgery often takes priority. Further, given that degenerative changes advance with age, the age differences between

Table 4. Partial Correlations between Metabolite Ratios and Radiological Parameters Controlled for Age and Height Effects

	HC group			*Patient group*		
	Volume	***CSA***	***CR***	***Volume***	***CSA***	***CR***
Mac/tNAA	–0.038	0.281	–0.047	–0.154	**–0.254**	**–0.275**
	$p=0.403$	$p=0.031$	$p=0.380$	$p=0.100$	$\mathbf{p=0.016}$*	$\mathbf{p=0.010}$*
tCr/tNAA	**0.329**	**0.302**	0.127	**–0.259**	**–0.343**	**–0.376**
	$\mathbf{p=0.014}$*	$\mathbf{p=0.022}$*	$p=0.203$	$\mathbf{p=0.014}$*	$\mathbf{p=0.002}$*	$\mathbf{p=0.001}$*
Glc + Tau/tNAA	0.002	0.085	0.213	–0.039	**–0.199**	–0.145
	$p=0.495$	$p=0.292$	$p=0.082$	$p=0.375$	$\mathbf{p=0.049}$*	$p=0.115$
Glx/tNAA	-0.173	-0.168	-0.002	**–0.277**	**–0.234**	**–0.205**
	$p=0.129$	$p=0.135$	$p=0.494$	$\mathbf{p=0.001}$*	$\mathbf{p=0.026}$*	$\mathbf{p=0.044}$*
myo-Ins/tNAA	0.226	**0.415**	0.054	**–0.277**	**–0.339**	**–0.278**
	$p=0.039$	$\mathbf{p=0.002}$*	$p=0.361$	$\mathbf{p=0.001}$*	$\mathbf{p=0.002}$*	$\mathbf{p=0.009}$*
tChol/tNAA	0.260	0.243	0.033	0.093	–0.078	–0.122
	$p=0.043$	$p=0.054$	$p=0.414$	$p=0.220$	$p=0.259$	p=0.154
CSA	**0.642**	n.a.	0.208	**0.684**	n.a.	**0.600**
	$\mathbf{p=0.000}$*		$p=0.085$	$\mathbf{p=0.000}$*		$\mathbf{p=0.025}$*
CR	–0.156	0.208	n.a.	**0.363**	**0.600**	n.a.
	$p=0.153$	$p=0.085$		$\mathbf{p=0.001}$*	$\mathbf{p=0.025}$*	

The asterisk represents the statistically significant result.

Mac, macromolecules; tNAA, total *N*-acetylaspartate; tCr, total creatine; Glc, glucose; Glx, combined glutamate/glutamine; myo-Ins, myo-inositol; tChol, total choline; CSA, cross-sectional area; CR, compression ratio; n.a., not applicable.

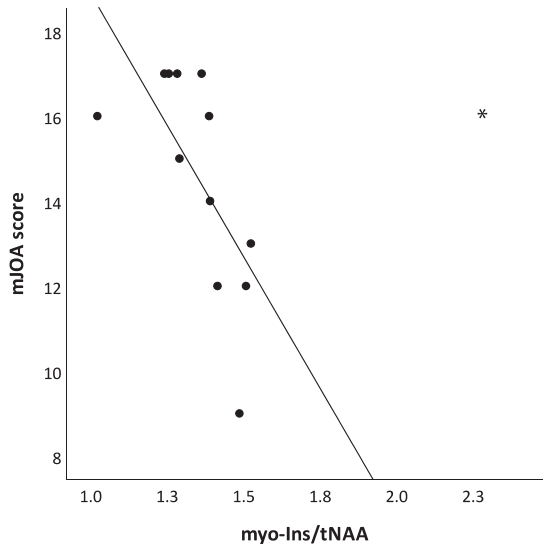

FIG. 5. Relationship between myo-Ins/tNAA and mJOA score, assessing the severity of degenerative cervical myelopathy ($N = 13$). The outlier (asterisk) was not included in the regression fit line. myo-Ins, myo-inositol; mJOA, modified Japanese Orthopedic Association (scale); tNAA, total *N*-acetylaspartate.

HC and DCM often appear in the literature.[14,17] Although the 4-year age difference between HC and DCM in this study did not reach the level of significance, the single-subject level analysis was corrected for the age effect. Age differences also declined when subjects were divided into groups according to compression severity. Despite the utilization of standard clinical MR hardware, there is still a need for operators trained in MRS data acquisition, post-processing, and relatively long acquisition times. These factors limit the use of the methodology herein at non-specialized centers. However, spinal MRS will gain from progress toward automatic MRS acquisition in the brain (e.g., user-independent voxel placement and power calibrations).[27]

Conclusion

In conclusion, the current study revealed neurochemical changes in CSC above the compression level in subjects with radiological signs of compression and clinical myelopathy and, for the first time, in non-myelopathic participants as well. State-of-the-art MRS demonstrated sufficient sensitivity to reveal early changes in non-myelopathic patients and thus might allow the stratification of non-myelopathic subjects. The current work warrants longitudinal studies assessing their risk of myelopathy development. Although MRS markers and level of spinal atrophy strongly reflected the severity of stenoses, volumes were less sensitive to clinical status than MRS.

Data availability statement

The data sets generated during the current study are not publicly available because of ethical reasons, but are available from the authors (petr.bednarik@meduniwien.ac.at, ts.horak@gmail.com) on reasonable request.

Acknowledgments

We thank Ing. Veronika Fabikova for her help with MRI data acquisition, Ing. Dagmar Kratochvilova for subject recruitment, Dr. Eva Koritakova for statistical analysis consultation, and Dr. Julien Cohen-Adad for providing valuable advice on data processing. Special thanks are due to the patients and healthy volunteers who participated in this study. Tony Long (Carsphairn, Scotland) helped work up the English.

Authors' Contributions

P.B., J.B., and T.H. are guarantors of the entire study. P.K. and P.B. set up the MR protocol. P.K. acquired the data. T.H. and P.B. analyzed the data. M.H., P.B., and A.S. performed the statistical analyses. T.H. and M.H. wrote the manuscript draft. Z.K. and Z.K.J. conducted the neurological assessment. J.V. processed the MRI data. T.R. and M.K. evaluated 1.5T MRI. E.V. carried out the electrophysiological evaluation. D.D. and P.G.H. provided technical expertise and adapted the sLASER pulse sequence (Oz and Tkac)[26] for spinal cord MRS. J.B., P.B., and T.H. coordinated the study. J.B., A.S., and P.B. designed the study. All authors contributed to interpreting the data, read and revised the manuscript, and agreed upon the final version.

Funding Information

This research was funded by Czech Health Research Council grants ref. NV18-04-00159 and by the Ministry of Health of the Czech Republic project for conceptual development in research organizations, ref. 65269705 (University Hospital, Brno, Czech Republic).

A.S. has received funding from the European Union's Horizon 2020 research and innovation program under a Marie Skłodowska-Curie grant agreement (no. 794986). P.B. was partially supported by the European Union's Horizon 2020 research and innovation program under a Marie Skłodowska-Curie grant agreement (no. 846793) and by a NARSAD Young Investigator Grant from the Brain and Behavior Research Foundation (no. 27238).

We acknowledge the core facility of the Multimodal and Functional Imaging Laboratory, Masaryk University, CEITEC supported by MEYS CR (LM2018129 Czech-BioImaging). Access to computing and storage facilities owned by parties and projects contributing to the National Grid Infrastructure MetaCentrum provided under the program ''Projects of Large Research, Development, and Innovations Infrastructures'' (CESNET LM2015042), is greatly appreciated.

The Center for Magnetic Resonance Research, University of Minnesota is supported, in part, by NIH Center grants P41EB027061 and P30NS076408.

Author Disclosure Statement

No competing financial interests exist.

Supplementary Material

Supplementary Table S1
Supplementary Table S2
Supplementary Table S3
Supplementary Figure S1
Supplementary Figure S2
Supplementary References

References

1. Gore, D.R., Sepic, S.B., and Gardner, G.M. (1986). Roentgenographic findings of the cervical spine in asymptomatic people. Spine 11, 521–524.
2. Kovalova, I., Kerkovsky, M., Kadanka, Z., Kadanka, Z., Nemec, M., Jurova, B., Dusek, L., Jarkovsky, J., and Bednarik, J. (2016). Prevalence and imaging characteristics of nonmyelopathic and myelopathic spondylotic cervical cord compression. Spine 41, 1908–1916.
3. Montgomery, D.M., and Brower, R.S. (1992). Cervical spondylotic myelopathy. clinical syndrome and natural history. Orthop. Clin. North Am. 23, 487–493.
4. Badhiwala, J.H., Ahuja, C.S., Akbar, M.A., Witiw, C.D., Nassiri, F., Furlan, J.C., Curt, A., Wilson, J.R., and Fehlings, M.G. (2020). Degenerative cervical myelopathy—update and future directions. Nat. Rev. Neurol. 16, 108–124.
5. Jutzeler, C.R., Ulrich, A., Huber, B., Rosner, J., Kramer, J.L.K., and Curt, A. (2017). Improved diagnosis of cervical spondylotic myelopathy with contact heat evoked potentials. J. Neurotrauma 34, 2045–2053.
6. Stroman, P.W., Wheeler-Kingshott, C., Bacon, M., Schwab, J.M., Bosma, R., Brooks, J., Cadotte, D., Carlstedt, T., Ciccarelli, O., Cohen-Adad, J., Curt, A., Evangelou, N., Fehlings, M.G., Filippi, M., Kelley, B.J., Kollias, S., Mackay, A., Porro, C.A., Smith, S., Strittmatter, S.M., Summers, P., and Tracey, I. (2014). The current state-of-the-art of spinal cord imaging: methods. Neuroimage 84, 1070–1081.
7. Martin, A.R., Aleksanderek, I., Cohen-Adad, J., Tarmohamed, Z., Tetreault, L., Smith, N., Cadotte, D.W., Crawley, A., Ginsberg, H., Mikulis, D.J., and Fehlings, M.G. (2016). Translating state-of-the-art spinal cord MRI techniques to clinical use: a systematic review of clinical studies utilizing DTI, MT, MWF, MRS, and fMRI. Neuroimage Clin. 10, 192–238.
8. Oz, G., Alger, J.R., Barker, P.B., Bartha, R., Bizzi, A., Boesch, C., Bolan, P.J., Brindle, K.M., Cudalbu, C., Dinçer, A., Dydak, U., Emir, U.E., Frahm, J., González, R.G., Gruber, S., Gruetter, R., Gupta, R.K., Heerschap, A., Henning, A., Hetherington, H.P., Howe, F.A., Hüppi, P.S., Hurd, R.E., Kantarci, K., Klomp, D.W.J., Kreis, R., Kruiskamp, M.J., Leach, M.O., Lin, A.P., Luijten, P.R., Marjańska, M., Maudsley, A.A., Meyerhoff, D.J., Mountford, C.E., Nelson, S.J., Pamir, M.N., Pan, J.W., Peet, A.C., Poptani, H., Posse, S., Pouwels, P.J.W., Ratai, E.-M., Ross, B.D., Scheenen, T.W., Schuster, C., Smith, I.C.P., Soher, B.J., Tkáč, I., Vigneron, D.B., and Kauppinen, R.A.; MRS Consensus Group. (2014). Clinical proton MR spectroscopy in central nervous system disorders. Radiology 270, 658–679.
9. Solanky, B.S., Abdel-Aziz, K., Yiannakas, M.C., Berry, A.M., Ciccarelli, O., and Wheeler-Kingshott, C.A. (2013). In vivo magnetic resonance spectroscopy detection of combined glutamate-glutamine in healthy upper cervical cord at 3 T. NMR Biomed. 26, 357–366.
10. Craciunas, S.C., Gorgan, M.R., Ianosi, B., Lee, P., Burris, J., and Cirstea, C.M. (2017). Remote motor system metabolic profile and surgery outcome in cervical spondylotic myelopathy. J. Neurosurg. Spine 26, 668–678.
11. Aleksanderek, I., McGregor, S.M.K., Stevens, T.K., Goncalves, S., Bartha, R., and Duggal, N. (2017). Cervical spondylotic myelopathy: metabolite changes in the primary motor cortex after surgery. Radiology 282, 817–825.
12. Holly, L.T., Ellingson, B.M., and Salamon, N. (2017). Metabolic imaging using proton magnetic spectroscopy as a predictor of outcome after surgery for cervical spondylotic myelopathy. Clin. Spine Surg. 30, E615–E619.
13. Holly, L.T., Freitas, B., McArthur, D.L., and Salamon, N. (2009). Proton magnetic resonance spectroscopy to evaluate spinal cord axonal injury in cervical spondylotic myelopathy. J. Neurosurg. Spine 10, 194–200.
14. Wyss, P.O., Huber, E., Curt, A., Kollias, S., Freund, P., and Henning, A. (2019). MR spectroscopy of the cervical spinal cord in chronic spinal cord injury. Radiology 291, 131–138.
15. Ellingson, B.M., Salamon, N., Hardy, A.J., and Holly, L.T. (2015). Prediction of neurological impairment in cervical spondylotic myelopathy using a combination of diffusion MRI and proton MR spectroscopy. PLoS One 10, e0139451.
16. Salamon, N., Ellingson, B.M., Nagarajan, R., Gebara, N., Thomas, A., and Holly, L.T. (2013). Proton magnetic resonance spectroscopy of human cervical spondylosis at 3T. Spinal Cord 51, 558–563.
17. Aleksanderek, I., Stevens, T.K., Goncalves, S., Bartha, R., and Duggal, N. (2017). Metabolite and functional profile of patients with cervical spondylotic myelopathy. J. Neurosurg. Spine 26, 547–553.
18. Karadimas, S.K., Erwin, W.M., Ely, C.G., Dettori, J.R., and Fehlings, M.G. (2013). Pathophysiology and natural history of cervical spondylotic myelopathy. Spine (Phila Pa 1976) 38, S21–S36.
19. Tetreault, L., Kopjar, B., Nouri, A., Arnold, P., Barbagallo, G., Bartels, R., Qiang, Z., Singh, A., Zileli, M., Vaccaro, A., and Fehlings, M.G. (2017). The modified Japanese Orthopaedic Association scale: establishing criteria for mild, moderate and severe impairment in patients with degenerative cervical myelopathy. Eur. Spine J. 26, 78–84.
20. Bednařík, J., Kadaňka, Z., Voháňka, S., Novotný, O., Šurelová, D., Filipovi-ová, D., and Prokeš, B. (1998). The value of somatosensory and motor evoked potentials in pre-clinical spondylotic cervical cord compression. Eur. Spine J. 7, 493–500.
21. Bednarik, J., Kadanka, Z., Dusek, L., Kerkovsky, M., Vohanka, S., Novotny, O., Urbanek, I., and Kratochvilova, D. (2008). Presymptomatic spondylotic cervical myelopathy: an updated predictive model. Eur. Spine J. 17, 421–431.
22. Kadanka, Z., Adamova, B., Kerkovsky, M., Kadanka, Z., Dusek, L., Jurova, B., Vlckova, E., and Bednarik, J. (2017). Predictors of symptomatic myelopathy in degenerative cervical spinal cord compression. Brain Behav. 7, e00797.
23. Joers, J.M., Deelchand, D.K., Lyu, T., Emir, U.E., Hutter, D., Gomez, C.M., Bushara, K.O., Eberly, L.E., and Öz, G. (2018). Neurochemical abnormalities in premanifest and early spinocerebellar ataxias. Ann. Neurol. 83, 816–829.
24. Gruetter, R., and Tkác, I. (2000). Field mapping without reference scan using asymmetric echo-planar techniques. Magn. Reson. Med. 43, 319–323.
25. Tkáč, I., Starčuk, Z., Choi, I.-Y., and Gruetter, R. (1999). In vivo 1H NMR spectroscopy of rat brain at 1 ms echo time. Magn. Reson. Med. 41, 649–656.
26. Oz, G., and Tkáč, I. (2011). Short-echo, single-shot, full-intensity proton magnetic resonance spectroscopy for neurochemical profiling at 4 T: validation in the cerebellum and brainstem. Magn. Reson. Med. 65, 901–910.
27. Öz, G., Deelchand, D.K., Wijnen, J.P., Mlynárik, V., Xin, L., Mekle, R., Noeske, R., Scheenen, T.W.J., and Tkáč, I.; Experts' Working Group on Advanced Single Voxel 1H MRS. (2020). Advanced single voxel 1 H magnetic resonance spectroscopy techniques in humans: experts' consensus recommendations. NMR Biomed. doi: 10.1002/nbm.4236.
28. De Leener, B., Lévy, S., Dupont, S.M., Fonov, V.S., Stikov, N., Louis Collins, D., Callot, V., and Cohen-Adad, J. (2017). SCT: Spinal Cord Toolbox, an open-source software for processing spinal cord MRI data. Neuroimage 145, 24–43.
29. Provencher, S.W. (1993). Estimation of metabolite concentrations from localized in vivo proton NMR spectra. Magn. Reson. Med. 30, 672–679.
30. Deelchand, D.K., Adanyeguh, I.M., Emir, U.E., Nguyen, T.-M., Valabregue, R., Henry, P.-G., Mochel, F., and Öz, G. (2015). Two-site reproducibility of cerebellar and brainstem neurochemical profiles with short-echo, single-voxel MRS at 3T. Magn. Reson. Med. 73, 1718–1725.
31. Bednařík, P., Henry, P.-G., Khowaja, A., Rubin, N., Kumar, A., Deelchand, D., Eberly, L.E., Seaquist, E., Öz, G., and Moheet, A. (2020). Hippocampal neurochemical profile and glucose transport kinetics in patients with type 1 diabetes. J. Clin. Endocrinol. Metab. 105, 479–491.
32. Cooke, F.J., Blamire, A.M., Manners, D.N., Styles, P., and Rajagopalan, B. (2004). Quantitative proton magnetic resonance spectroscopy of the cervical spinal cord. Magn. Reson. Med. 51, 1122–1128.
33. Hock, A., Fuchs, A., Boesiger, P., Kollias, S.S., and Henning, A. (2013). Electrocardiogram-triggered, higher order, projection-based B0 shimming allows for fast and reproducible shim convergence in spinal cord 1H MRS. NMR Biomed. 26, 329–335.

34. Hock, A., Henning, A., Boesiger, P., and Kollias, S.S. (2013). (1)H-MR spectroscopy in the human spinal cord. AJNR Am. J. Neuroradiol. 34, 1682–1689.
35. Dydak, U., Kollias, S., Schär, M., Meier, D., and Boesiger, P. (2005). MR spectroscopy in different regions of the spinal cord and in spinal cord tumors. Presented at thye Proceedings of the Annual Meeting of the International Society of Magnetic Resonance in Medicine, Miami Beach, FL.
36. Nouri, A., Martin, A.R., Mikulis, D., and Fehlings, M.G. (2016). Magnetic resonance imaging assessment of degenerative cervical myelopathy: a review of structural changes and measurement techniques. Neurosurg. Focus 40, E5.
37. Grabher, P., Mohammadi, S., David, G., and Freund, P. (2017). Neurodegeneration in the spinal ventral horn prior to motor impairment in cervical spondylotic myelopathy. J. Neurotrauma 34, 2329–2334.
38. Qian, J., Herrera, J.J., and Narayana, P.A. (2010). Neuronal and axonal degeneration in experimental spinal cord injury: in vivo proton magnetic resonance spectroscopy and histology. J. Neurotrauma 27, 599–610.
39. Heckova, E., Strasser, B., Hangel, G.J., Považan, M., Dal-Bianco, A., Rommer, P.S., Bednarik, P., Gruber, S., Leutmezer, F., Lassmann, H., Trattnig, S., and Bogner, W. (2019). 7 T magnetic resonance spectroscopic imaging in multiple sclerosis: how does spatial resolution affect the detectability of metabolic changes in brain lesions? Invest. Radiol. 54, 247–254.
40. Carew, J.D., Nair, G., Pineda-Alonso, N., Usher, S., Hu, X., and Benatar, M. (2011). Magnetic resonance spectroscopy of the cervical cord in amyotrophic lateral sclerosis. Amyotroph. Lateral Scler. 12, 185–191.
41. Lenglet, C., Joers, J., Pisharady, P., Deelchand, D., Hutter, D., and Bushara, K. (2016). Cross-sectional and longitudinal diffusion MRI and MRS of the spinal cord in Friedreich's Ataxia. Presented at OHBM 2016: 22nd Annual Meeting of the Organization for Human Brain Mapping, Rome.
42. Grabher, P., Mohammadi, S., Trachsler, A., Friedl, S., David, G., Sutter, R., Weiskopf, N., Thompson, A.J., Curt, A., and Freund, P. (2016). Voxel-based analysis of grey and white matter degeneration in cervical spondylotic myelopathy. Sci. Rep. 6, 24636.